

In vitro Bioactivity and Gene Silencing Effect of shRNA-VEGF Loaded Chitosan Nanoparticles

Murat Doğan 

¹Sivas Cumhuriyet University, Faculty of Pharmacy, Sivas, Türkiye

ABSTRACT:

Purpose: In this study, it is aimed to prepare chitosan nanoparticles including shRNA-VEGF and evaluate their bioactivity by *in vitro* cell culture studies and to perform mechanical characterization of nanoparticles.

Material and Methods: Ionic chelation method was used to prepare nanoparticles. The XTT assay was used to assess the cytotoxic activity of shRNA-VEGF and shRNA-VEGF loaded NP on the HeLa and NIH 3T3 cells.

Results: IC₅₀ values of shRNA-VEGF and NP including shRNA-VEGF were assessed. IC₅₀ values of shRNA-VEGF and NP including shRNA-VEGF were 0.89±0.010 and 0.52±0.004 µg/mL on HeLa cells. Bax amounts of control, shRNA-VEGF, and shRNA-VEGF loaded NP was calculated as 23.70±0.27, 34.64±0.36, and 39.46±0.54 ng/mg protein, respectively. The findings showed that cleaved caspase 3 amounts of control, shRNA-VEGF, and shRNA-VEGF containing NP was calculated as 711.70±4.40, 767.23±3.82, and 825.32±5.06 pg/mg protein.

Conclusion: While producing no cytotoxicity in NIH 3T3 cells, shRNA-VEGF and shRNA-VEGF loaded NP substantially inhibited HeLa cell reproduction depending on the concentration. By using shRNA-VEGF and shRNA-VEGF loaded NP, the expression of pro-apoptotic Bax and cleaved caspase 3 proteins was considerably elevated.

Keywords: shRNA-VEGF, Nanoparticle, RNA interference, Cell viability, ELISA kits

Corresponding author: Murat Doğan, email: mdogan@cumhuriyet.edu.tr

INTRODUCTION

Cancer is the second most common reason of mortality and is a serious health issue. Every system and organ in the body develops a unique collection of maladies as a result of cancer, which is both a sickness and a group of illnesses (Docea et al., 2012; Salehi et al., 2019). Smoking, living a healthy lifestyle, and eating habits all contribute to about one-third of cancer fatalities. In addition, changing bad lifestyle practices can help prevent a number of malignancies (Ghad et al., 2014; Sharifi-Rad et al., 2020). The conventional therapeutic modalities and tools utilized in the medication for cancer include surgery, chemotherapy, immunotherapy, radiation and targeted treatment (Jovčevska and Muyltermans

2020; Park, Heo and Han 2018). These methods typically have negative consequences and carry a high chance of recurrence. Some of the most common adverse effects include neuropathies, skin, gastrointestinal. Because conventional cancer treatment strategies entail the aforementioned negative effects, new treatment strategies are being researched (Wang, Billone and Mullett 2013; Zitvogel et al., 2008). The treatment of cancer with nanotechnology-based drug delivery systems is promising, and these studies are at the forefront of the field (Adair, Parette and Altinoglu 2010; Altinoglu and Adair 2010). Biocompatibility, high bioavailability, simple tumor targeting, and diminished or eliminated negative effects are only a

few advantages of nanoparticulate delivery systems. (Mansoori et al., 2017; Wang, Zhang and Chen 2019). The major ways that anti-cancer nanomedicine can provide anti-cancer efficacy are by raising the quantity of cytotoxic medications in tumor areas, which boosts anti-cancer activity (Longacre, Snyder and Sarkar 2014; Xue and Liang 2012), reducing its clearance, minimizing side effects in healthy organs, minimizing undesired toxicity, and simultaneously transporting a number of anti-cancer active chemicals (Mittal et al., 2020; Robey et al., 2018; Singh, Benjakul and Prodpran 2019a).

According to these characteristics, RNA interference (RNAi), a posttranscriptional gene control mechanism based on double-stranded RNA, represents a novel class of potential therapeutics (Demolin and Essaqrir 2014; Urban-Klein, Werth and Abuharbeid 2005). On the other hand, therapeutic application of RNAi molecules is constrained and a suitable delivery mechanism is required because of fast breakdown of nucleases, biological lability, ineffective cellular absorption, and off-target effects (Howard et al., 2009). Even while viral vectors are often employed as delivery systems, there are a number of drawbacks, such as immunological reaction and carcinogenic effect, and as a result, nonviral vectors are becoming more and more common. Publications on the impact of VEGF /VEGF R on tumor angiogenesis have appeared in recent years. The growth factor family that includes VEGFs consists of various disulfide-linked dimers. Most cells use VEGF molecules as mitogens, and their expression rises in several cancerous conditions. In recent years, it has been discussed that the vascular endothelial growth factor (VEGF) signaling pathway differs in normal and cancer cells (Howard et al., 2009). Due to its biodegradability, biocompatibility, and low toxicity, chitosan, a deacetylated (DA) chitin derivative, is frequently used in the pharmaceutical and medical industries (Li, Cai and Ja 2018; Singh, Benjakul and Prodpran 2019b). Additionally, it can be utilized as a means of delivering medications, a packaging material, an antibacterial agent, a tissue engineering tool, an anti-aging agent, an antibody response enhancer, and for the treatment of diseases like cancer (Bhattarai, Gunn and Zhang 2010; Torabi et al., 2018; Jhaveri et al., 2021). It is

frequently employed in nano applications, including as the delivery of pharmaceuticals. Specific types of cancer cells have been demonstrated to be less prone to proliferating, differentiating, and surviving when exposed to shRNA-VEGF, which works by concentrating on key substances that promote tumor cell growth (Cheimonidi et al., 2018; Tavana et al., 2020). This substance was chosen for the investigation because shRNA-VEGF has antioxidant and anti-proliferative properties.

In this test, shRNA-VEGF was enclosed in cationic polymer chitosan nanoparticles, which are a biocompatible and biodegradable material. The impact of shRNA-VEGF and shRNA-VEGF nanoparticles (NPs) on NIH 3T3 and HeLa cells were examined in XTT and bioactivity tests. In this work, the levels of BCL-2, cleaved caspase 3, and Bax in shRNA-VEGF, shRNA-VEGF loaded NPs administered, and non-administered HeLa cells were measured using human ELISA kits. In order to determine the appropriateness and usability of shRNA-VEGF NPs in XTT and biological activity experiments, the requisite characterization tests on nanoparticles were also carried out.

MATERIAL and METHODS

Cell culture studies

HeLa and NIH 3T3 cells were obtained ATCC for the cytotoxic activity investigation. Merck Millipore supplied the fetal bovine serum (FBS), shRNA-VEGF, and DMEM. PBS, polyvinyl pyrrolidone (PVP), and chitosan (400 kDa, DD 92) were purchased from Sigma-Aldrich. Studies on cytotoxic effect used the XTT reagent from Roche Diagnostic. Cells were grown in well plates inside of an incubator at 37 °C and 5% CO₂. Cells have to be at least 80% confluent for the cytotoxic activity assays to be completed (Taskin et al., 2020). The following equation was then used to calculate cell viability.

$$\text{Cell viability (\%)} = \frac{\text{Absorbance of sample}}{\text{Absorbance of control}} \times 100 \quad (1)$$

Preparation of chitosan NPs

NPs carrying shRNA-VEGF were made using the ionic gelation technique. Chitosan was dissolved in acetic acid (0.5% v/v) in the appropriate amount while

being magnetically agitated at 1000 rpm (Calvo et al., 1997; Wikanta et al., 2012). PVP was dissolved in sterile deionized water (0.25% w/v) at a preset concentration. The PVP solution containing shRNA-VEGF is added to the chitosan solution (0.5% w/v). The NP suspension for 30 minutes while centrifuging it at 10,000 rpm. The NPs' loading capacity (LC) and encapsulation efficiency (EE) were assessed by removing the supernatant and separating a 1 mL sample from it. The pellet was afterward cleaned with deionized water. The pellet was centrifuged 15 minutes at 10,000 rpm after being combined with 30 mL of deionized water. This procedure was carried out twice. Lyophilized NPs maintained at +4 °C.

EE and LC studies of NPs

shRNA-VEGF in NPs was measured using an UV vis spectrophotometer to determine its EE % and LC % (Tavana et al., 2020). By measuring the absorbance of shRNA-VEGF at different concentration at 380 nm a spectral line equation was created. The line equation was used to determine how much shRNA-VEGF was present in the supernatant. The LC and EE of the NPs were calculated using the following equations (2, 3).

$$EE (\%) = \frac{(m_o - m_s)}{m_o} \times 100 \quad (2)$$

$$LC (\%) = \frac{(m_o - m_s)}{w_{np}} \times 100 \quad (3)$$

w_{np} = total weight of shRNA-VEGF in NPs, m_o is starting mass of shRNA-VEGF, m_s is the amount of shRNA-VEGF in the supernatant, and m_o is the first mass of shRNA-VEGF (Taskin et al., 2020). Every measurement was made in tri times, and the results shown as mean SEM.

Assessment of particle size and zeta (ζ) potential

A device called the Zetasizer Nano ZS was utilized to assess the size and ζ potential measurements of NPs (Taşkın et al., 2021). NPs assessed while suspended in PBS (pH 7.4).

In vitro release study of NPs

shRNA-VEGF was released *in vitro* from chitosan NPs in PBS (pH 7.4) using the same procedures as

described in the release experiment (Calvo et al., 1997; Wikanta et al., 2012). The shRNA-VEGF-loaded NPs were initially diluted buffer solution (2 mL) and kept in an agitated water bath at 25 °C. Samples were centrifuged at 10000 rpm for 10 min at 25 °C at preset intervals. In order to keep the total volume constant and for analysis, 800 μ l of the supernatant were taken out, and an equivalent volume of the fresh buffer put in their place. Using a UV-vis spectrophotometer, the quantity of released shRNA-VEGF at a certain moment was calculated.

Cell viability assay

The XTT study was performed to assess the cytotoxic activity of shRNA-VEGF and shRNA-VEGF loaded NP on the HeLa and NIH 3T3 cells. DMEM (100 L, 10% FBS) was first used to seed cells in 96-well plates, and the cells were then left to incubate overnight (Han et al., 2015; Gömeç et al., 2022; Keawchaon and Yoksan 2011; Mohammadi, Hashemi and Hosseini 2015; Purbowatiningrum and Ismiyanto 2017). After that, cells were exposed to shRNA-VEGF and shRNA-VEGF loaded NP at a range of doses (0.25, 0.5, 1, 2, and 5 μ g/mL) for 24 hours. The samples were added to each well after being pipetted and vortexed in DMEM to homogenize them. Plates with cells and samples were then incubated for 24 hours. After this time, wells were cleaned PBS (200 μ L). Each well received 100 μ L of colorless DMEM and 50 μ L of XTT, and the cells were then incubated for 4 hours. The absorbance of XTT-formazan at 450 nm was measured by a ELISA reader. On the HeLa and NIH 3T3 cells, the cell viability and IC₅₀ values of shRNA-VEGF and shRNA-VEGF loaded NP were calculated.

The assessment of BCL-2, cleaved caspase 3, and Bax amounts

The levels of BCL-2, cleaved caspase 3, and Bax in shRNA-VEGF, shRNA-VEGF loaded NPs treated, and untreated HeLa cells were determined using the human ELISA kits of cleaved caspase 3, BCL-2, and Bax. HeLa cells were first placed in a 6-well plate with DMEM and treated for 24 hours with 1 g/mL shRNA-VEGF and shRNA-VEGF loaded NP. shRNA-VEGF and NP, including shRNA-VEGF, were applied to HeLa cells, and those that were not were collected and diluted in PBS. They were then duplicated, frozen,

and thawed. In accordance with the manufacturer's instructions, the amounts of cleaved caspase 3, BCL-2, and Bax in cell lysates were then measured. The total protein amounts in shRNA-VEGF and shRNA-VEGF loaded NP untreated and treated HeLa cells were calculated using the Bradford protein assay kit (Merck Millipore, Darmstadt, Germany).

Total oxidant status (TAS) and Total antioxidant status (TOS) measurements in shRNA-VEGF and NP including shRNA-VEGF treated and untreated HeLa cells

The amounts of TAS and TOS in shRNA-VEGF and NP including shRNA-VEGF treated and untreated HeLa cells, were assessed using the total antioxidant and oxidant status assay kit (Rel Assay Diagnostics, Turkey) (Doğan ve Karademir 2020). 1 µg/mL shRNA-VEGF and shRNA-VEGF NP were applied to HeLa cells for 24 hours. Data were presented for TAS and TOS as mol H₂ O₂ Equiv./L and mmol Trolox Equiv./L, respectively.

Participant and sampling

MD carried out research and data analysis. MD oversaw the entire undertaking and created the experiments. MD drafted the article, read it, and gave his approval to the final manuscript.

Statistical Analysis

One-way ANOVA and repeated measures ANOVA were used to analyze the results, and a Tukey post hoc test was used for multiple comparisons between

groups. A mean and SEM are used to present all results. The threshold for significance was set at **p< 0.05.

Ethical Approval

Not applicable.

RESULTS

EE and LC of NP including shRNA-VEGF

shRNA-VEGF content in chitosan NPs is shown by the EE rate. EE and LC values are very important in cell culture studies in terms of transfection efficiency. The findings of the calculation used to determine the rate of shRNA-VEGF encapsulated into chitosan NP are displayed in Table 1. The findings showed that the computed EE value of NPs containing shRNA-VEGF was 79.52±0.03 %. Additionally, LC of NPs was found to be 7.93±0.03 %. The findings support the conclusion that shRNA-VEGF 's EE and LC values of NPs were appropriate for cell culture and bioactivity research.

Characterization of NPs

The findings of the evaluation of NPs particle size, potential, and polydispersity index (PDI) are shown in Table 2. The NP's dimensions were 178.34±2.10 nm. The NP's ζ potential was detected at as 1.52±0.03 mV. Additionally, the PDI ratio of NP was 0.204±0.03. Three repeats of each measurement were carried out. The findings suggest that NP was composed of homogeneous features with no aggregation.

Table 1 EE and LC of shRNA-VEGF loaded NPs

Parameter	ShRNA-VEGF
Linear equation	y=0.2704 x±0.0197
Slope±SD	0.2704±0.021
Intercept	0.0197±0.0010
R	0.9864
EE %	79.52±0.03
LC %	7.93±0.03

Table 2. ζ potential, particle size, and PDI values of shRNA-VEGF -loaded NP

Samples	ζ potential (mV) ± SD	Size (nm) ± SD	PDI ± SD
*NP	1.52±0.03	178.34±2.10	0.204±0.03

* NP contains chitosan, shRNA-VEGF and, PVP

In vitro release kinetics study result of NP with shRNA-VEGF loaded

At 37 °C for 288 hours, the release profile of shRNA-VEGF from NP was examined (Fig. 1). 0.1 M PBS was utilized in this study to mimic physiological circumstances. The shRNA-VEGF release data demonstrated a regulated release with a quick first release (50%) in 24 hours, afterward a constant and gradual release (75%) until 144 hours. In just 288

hours, nearly all of the shRNA-VEGF (99,65%) in the NP was released. In research of acetylsalicylic acid, this kind of constant and gradual release was noted. The shRNA-VEGF is released from the NP mostly as a result of diffusion and molecular matrix erosion. shRNA-VEGF can readily diffuse from the NP's pores or surface since its size is less than the particle (Purbowatiningrum and Ismiyanto 2017; Tang et al., 2018).

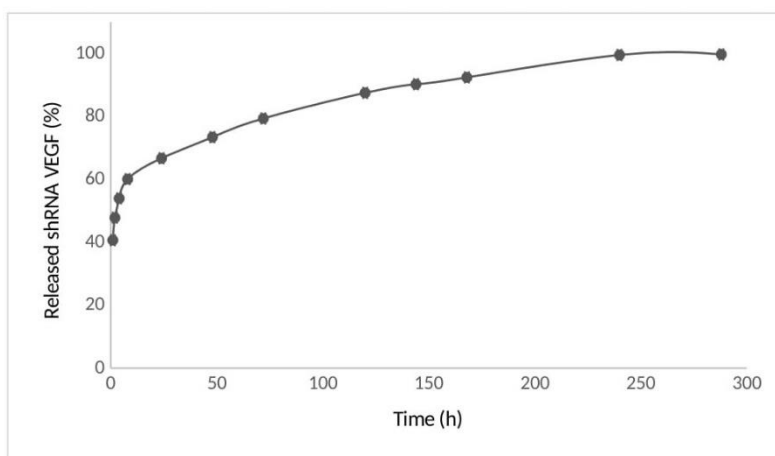


Figure 1. Release kinetics of shRNA-VEGF loaded NP in 0.1 M PBS (pH 7.4). By accumulating cumulative over time, the release rate of shRNA-VEGF was estimated.

Assessment of cytotoxic activity results

HeLa and NIH 3T3 cells were treated to evaluate the IC_{50} values of shRNA-VEGF and NP containing shRNA-VEGF at predetermined doses. Both shRNA-VEGF and the shRNA-VEGF loaded NP considerably reduced HeLa cell viability, according to the findings of the XTT investigation, depending on the dose and IC_{50} values were indicated Table 3. Cell viability were estimated as $63.06 \pm 0.51\%$ and $59.01 \pm 0.42\%$, respectively, when the sole shRNA-VEGF and NP were treated with HeLa cells at 0.25 g/mL concentration. HeLa cells were exposed to the greatest dose of shRNA-VEGF (5 g/mL), and cell viability were assessed to be $29.67 \pm 0.18\%$ and $22.74 \pm 0.21\%$, respectively. The shRNA-VEGF loaded NP demonstrated more potent (** $p < 0.05$, Table 3) cytotoxic activity at all concentrations of shRNA-VEGF and shRNA-VEGF loaded NP treated with the cells, in accordance with the findings of the cytotoxic activity investigation conducted on HeLa cells. These

results were used to calculate the IC_{50} values for shRNA-VEGF and NP containing shRNA-VEGF. On the HeLa cell line, the IC_{50} values for shRNA-VEGF and NP containing shRNA-VEGF were 0.89 ± 0.010 and 0.52 ± 0.004 $\mu\text{g/mL}$, respectively. According to the findings, the shRNA-VEGF loaded NP exhibits greater cytotoxic effect in HeLa cells and a lower IC_{50} value than the shRNA-VEGF alone.

A percentage of viable cells compared to the control group is used to represent the results. The information is displayed as a mean and SEM. In comparison to the control group, both quantities of shRNA-VEGF and shRNA-VEGF loaded NP significantly inhibited the proliferation of HeLa cells. The shRNA-VEGF and the NP incorporating shRNA-VEGF were administered NIH 3T3 cells at 0.25 $\mu\text{g/mL}$ concentration, and the results of the NIH 3T3 cell viability were indicated (Table 3) and the cell viability was determined as $87.06 \pm 0.51\%$ and $90.38 \pm 0.42\%$. The cell viability of NIH 3T3 cells after administration

of shRNA-VEGF and the shRNA-VEGF loaded NP was determined to be $81.30 \pm 0.11\%$ and $84.86 \pm 0.08\%$, respectively. When NIH 3T3 cells were treated with shRNA-VEGF and the NP with shRNA-VEGF, the cell viability was estimated to be $74.68 \pm 0.18\%$ and $77.40 \pm 0.23\%$, respectively, at $5 \mu\text{g/mL}$

concentration. The findings show that it was difficult to estimate the IC_{50} values of the shRNA-VEGF and NP containing the shRNA-VEGF at the indicated doses. On NIH 3T3 cells, shRNA-VEGF and shRNA-VEGF loaded NP were both biocompatible and non-cytotoxic.

Table 3. The cytotoxic activity of shRNA-VEGF and shRNA-VEGF loaded NP on HeLa cell line.

Samples/Concentrations	HeLa cell viability (% of control)				
	0.25 $\mu\text{g/mL}$	0.5 $\mu\text{g/mL}$	1 $\mu\text{g/mL}$	2 $\mu\text{g/mL}$	5 $\mu\text{g/mL}$
shRNA-VEGF	63.06 ± 0.51	55.03 ± 0.18	46.69 ± 0.36	37.78 ± 0.42	29.67 ± 0.29
shRNA-VEGF NP	59.08 ± 0.42	51.03 ± 0.32	40.03 ± 0.40	31.89 ± 0.28	22.74 ± 0.27

Table 4. The anti-proliferative activity of shRNA-VEGF and the NP including shRNA-VEGF on NIH 3T3 cell line. In comparison to the control group, the results are shown as a percentage of viable cells.

Samples/Concentrations	NIH 3T3 cell viability (% of control)				
	0.25 $\mu\text{g/mL}$	0.5 $\mu\text{g/mL}$	1 $\mu\text{g/mL}$	2 $\mu\text{g/mL}$	5 $\mu\text{g/mL}$
shRNA-VEGF	87.06 ± 0.51	81.30 ± 0.11	80.69 ± 0.33	77.78 ± 0.42	74.68 ± 0.18
shRNA-VEGF NP	90.38 ± 0.42	84.86 ± 0.08	82.03 ± 0.35	79.89 ± 0.28	77.40 ± 0.23

The effect of shRNA-VEGF and shRNA-VEGF NPs on BCL-2, cleaved caspase 3, and Bax quantities in HeLa cells

Bax, cleaved caspase 3, and BCL-2 were among the proteins whose expression was evaluated by ELISA in HeLa cells. Bax amount was considerably enhanced after 24 hours of treatment with shRNA-VEGF and shRNA-VEGF-loaded NP ($1 \mu\text{g/mL}$) (** $p < 0.05$, Table 4). In accordance with the findings, the amounts of Bax in the control, shRNA-VEGF, and shRNA-VEGF loaded NP were 23.70 ± 0.27 , 34.64 ± 0.36 , and 39.46 ± 0.54 ng/mg protein, respectively. The measurements showed that cleaved caspase 3

quantity amounts in the control, shRNA-VEGF, and shRNA-VEGF-loaded NP were 711.70 ± 4.40 , 767.23 ± 3.82 , and 825.32 ± 5.06 pg/mg protein, respectively. The measurements of BCL-2 concentrations in the control, shRNA-VEGF, and shRNA-VEGF NP were 43.22 ± 0.38 , 42.22 ± 0.28 , and 40.15 ± 0.60 ng/mg protein, respectively (Table 5). Results indicated shRNA-VEGF and shRNA-VEGF loaded NP significantly increased the quantity of cleaved caspase 3 on HeLa cells. However, shRNA-VEGF and shRNA-VEGF loaded NP had no activity against BCL-2 amount ($p > 0.05$).

Table 5. shRNA-VEGF and shRNA-VEGF loaded NP enhanced apoptosis in HeLa cells at a dose of $1 \mu\text{g/mL}$.

Samples	Bax (ng/mg)	cleaved caspase 3 (pg/mg)	BCL-2 (ng/mg)
Control	23.70 ± 0.27	711.70 ± 4.40	43.22 ± 0.38
shRNA-VEGF	34.64 ± 0.36	767.23 ± 3.82	42.22 ± 0.28
shRNA-VEGF NP	39.46 ± 0.54	825.32 ± 5.06	40.15 ± 0.60

The quantities of BAX, BCL-2, and cleaved Caspase 3 were determined using ELISA kits. Each result is shown as a mean and SEM. ShRNA-VEGF and shRNA-

VEGF-loaded NP show no possible impact on BCL-2 expression, which is anti-apoptotic.

The effect of shRNA-VEGF and shRNA-VEGF loaded NPs on TAS and TOS amounts in HeLa cells

Using a TAS and TOS assay kit, the impact of shRNA-VEGF and shRNA-VEGF loaded NP on the levels of TAS and TOS in HeLa cells was examined. TAS amount was unaffected by either shRNA-VEGF or shRNA-VEGF loaded NP ($p>0.05$). Additionally, HeLa cells' TOS production was boosted by the shRNA-

VEGF and shRNA-VEGF loaded NP ($p<0.05$). TAS values for the control, shRNA-VEGF, and shRNA-VEGF loaded NP were 0.584 ± 0.018 $\mu\text{g/mL}$, 0.563 ± 0.016 , and 0.572 ± 0.011 $\mu\text{g/mL}$, respectively. Furthermore, the TOS values for control, shRNA-VEGF, and shRNA-VEGF loaded NP were 34.946 ± 0.281 $\mu\text{g/mL}$, 42.336 ± 0.550 , and 50.276 ± 0.589 $\mu\text{g/mL}$, respectively (Fig. 2).

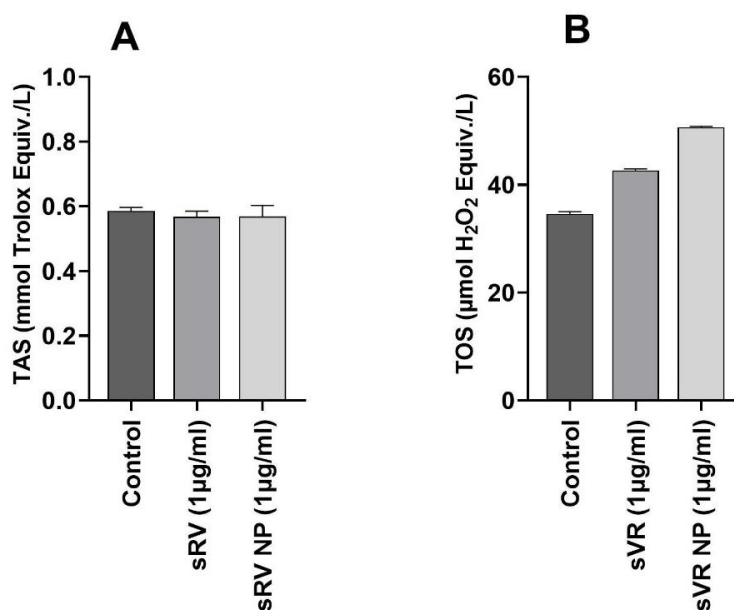


Figure 2. The TAS level (A) of HeLa cells was not significantly altered by the addition of shRNA-VEGF or shRNA-VEGF loaded NP at a concentration of 1 $\mu\text{g/mL}$, however the TOS level (B) was significantly raised.

DISCUSSION

While the using contemporary chemotherapy and radiotherapy during the cancer treatment, drug resistance, relapse, and metastasis have hindered the treatment of cervical cancer in several countries both developing and developed worldwide. Among its bioactive properties, shRNA-VEGF has antioxidant and anti-cancer properties. shRNA-VEGF and shRNA-VEGF NP showed cytotoxic effect on HeLa cells depending on concentration. With IC_{50} values of shRNA-VEGF and NP of 0.89 ± 0.010 and 0.52 ± 0.004 $\mu\text{g/mL}$ on HeLa cells, it significantly inhibited HeLa cell reproduction after 24 hours depending on concentration. Compared to control and shRNA-VEGF, NP containing shRNA-VEGF, in particular, had a substantially more antiproliferative activity against HeLa cells. The cytotoxic effects of

shRNA-VEGF and NP loaded with shRNA-VEGF against NIH 3T3 cells were examined in this situation, and the findings indicated that shRNA-VEGF and NP had no cytotoxic impact on NIH 3T3 cells. It is well known that apoptosis affects the effectiveness of pharmacological treatments and plays a role in the cellular growth of tumors (Chen, 2013). By measuring the amounts of BCL-2 and Bax by ELISA, it was possible to verify that shRNA-VEGF had an apoptotic effect on HeLa cells. As one of the defenses against the creation and proliferation of tumors is the beginning of cell apoptosis, which is a primary goal of cancer treatment (Sachdev et al., 2019). Both apoptotic proteins are found in the BCL-2 protein family, and the proportion of pro- to anti-apoptotic proteins is frequently used to predict the destiny of cells. When Bax tears apart the mitochondrial

membrane and cytochrome c releasing, the apoptosome complex is created. This combination stimulates caspases and causes apoptosis. Moreover, BCL2 maintains membrane integrity, inhibits the release of cytochrome c, and inhibits apoptosis (Sima, Richter and Vetvicka 2019). The activation of caspases is a crucial aspect of the process (Chen, Zhang and Gao 2018; Guo et al., 2016; Lee et al., 2019). In this work, 1 µg/mL shRNA-VEGF and shRNA-VEGF loaded NP dramatically boosted the expression of the proteins Bax and cleaved caspase 3, but had no apparent influence on the expression of the anti-apoptotic BCL-2. The amount of Bax and caspase 3 was significantly increased in shRNA-VEGF loaded NP samples when compared to shRNA-VEGF alone and the control group. Bax and cleaved caspase 3 levels dramatically increased in HeLa cells after treatment with 2 µg/mL concentrations of shRNA-VEGF and shRNA-VEGF loaded NP, indicating that these substances had cytotoxic and apoptotic effects. Most anti-cancer medications study inducing the majority of macromolecular changes in cells are assumed to be caused by oxidative stress in tumor cells. TOS, one of the many metrics used to gauge oxidative stress, is widely employed to assess the general level of oxidative stress in cells. The TAS is also used to evaluate the antioxidant capacity of cells. By elevating TOS levels, we aimed to determine whether shRNA-VEGF and shRNA-VEGF loaded NP may produce cytotoxicity. shRNA-VEGF and shRNA-VEGF loaded NP administration over 24 hours increased TOS levels in comparison to untreated cells, but TOS levels were not significantly different. Treatment with shRNA-VEGF and shRNA-VEGF loaded NP raised TOS while having no impact on TOS, showing that oxidative stress was induced in the shRNA-VEGF and shRNA-VEGF loaded NP treated HeLa cells. The mitochondrial membrane can be damaged, and an excessive spike in reactive oxygen species can also cause the intrinsic apoptotic pathway to be activated. (Filiz, Joha and Yulak 2021; Lee et al., 2019).

CONCLUSION

NIH 3T3 cells were not harmed by the presence of shRNA-VEGF or shRNA-VEGF loaded NP, while HeLa

cell proliferation was drastically inhibited in a concentration-dependent manner. By using shRNA-VEGF and shRNA-VEGF loaded NP, it was possible to greatly boost the expression of pro-apoptotic Bax and cleaved caspase 3 proteins. An increase in TOS supported the cytotoxic effects of shRNA-VEGF and shRNA-VEGF loaded NP. ShRNA-VEGF and shRNA-VEGF loaded NP have the potential to be a novel and efficient anticancer strategy due to their encouraging results in the suppression of cancer cells and lack of damage in healthy cells.

Acknowledgment

This study was performed at own expense in Cumhuriyet University.

Conflict of Interest

The author declare that they have no conflict of interest.

REFERENCES

- Adair, J.H., Parette, M.P., Altinoglu, E.I. (2010). Nanoparticulate alternatives for drug delivery. *ACS Nano.*, 4(9), 4967-4970. <https://dx.doi.org/doi:10.1021/nn102324e>.
- Altinoglu, E.I., Adair, J.H. (2010). Near infrared imaging with nanoparticles. *Wiley Interdiscip. Rev. Nanomed. Nanobiotechnol.*, 2(5), 461-477. <https://dx.doi.org/doi:10.1002/wnan.77>
- Bhattacharai, N., Gunn, J., Zhang, M. (2010). Chitosan-based hydrogels for controlled, localized drug delivery. *Adv Drug Deliv Rev.*, 62(1), 83-99. <https://dx.doi.org/doi:10.1016/j.addr.2009.07.019>.
- Calvo, P., Remunan-Lopez, C., Vila-Jato, J.L. et al. (1997). Novel hydrophilic chitosan-polyethylene oxide nanoparticles as protein carriers. *J Appl Polym Sci.*, 63(1), 125-132. [https://doi.org/10.1002/\(SICI\)1097-4628](https://doi.org/10.1002/(SICI)1097-4628)
- Cheimonidi, C., Samara, P., Polychronopoulos, P. et al. (2018). Selective cytotoxicity of the herbal substance acteoside against tumor cells and its mechanistic insights. *Redox Biol.*, 16, 169-178. <https://dx.doi.org/doi:10.1016/j.redox.2018.02.015>.
- Chen, Z., Zhang, B., Gao, F. et al. (2018). Modulation of G2/M cell cycle arrest and apoptosis by luteolin in human colon cancer cells and xenografts. *Oncol Lett.*, 15, 1559-1565. <https://doi.org/10.3892/ol.2017.7475>.
- Chen, J. (2013). Recent advance in the studies of β-glucans for cancer therapy. *Anticancer Agents Med Chem.*, 13, 679-80. <https://dx.doi.org/doi:10.2174/1871520611313050001>
- Demoulin, J., Essaahir, A. (2014). PDGF receptor signaling networks in normal and cancer cells. *Cytokine Growth Factor Rev.*, 25, 273-83. <https://dx.doi.org/doi:10.1016/j.cytog.2014.05.001>

- 10.1016/j.cytogfr.2014.03.003.
- Docea, A.O., Mitrut, P., Grigore, D. et al. (2012). Immunohistochemical expression of TGF beta (TGF-beta), TGF beta receptor 1 (TGFBR1), and Ki67 in intestinal variant of gastric adenocarcinomas. *Rom J Morphol Embryol*, 53(3), 683-92. <https://dx.doi.org/10.23188426>
- Doğan, M., Karademir, M. (2020). Effect of captopril on the oxidative damage caused by pentylenetetrazole in the SHSY-5Y human neuroblastoma cell line. *Cumhuriyet Medical Journal*, 42(4), 479-483. <https://doi.org/10.7197/cmj.830835>.
- Filiz, A.K., Joha, Z., Yulak, F. (2021). Mechanism of anti-cancer effect of β -glucan on HELA cell line. *Bangladesh Journal of Pharmacology*, 16(4), 122-128. <https://doi.org/doi:10.3329/bjp.v16i4.54872>
- Ghad, A., Mahjoub, S., Tabandeh, F. et al. (2014). Synthesis and optimization of chitosan nanoparticles: potential applications in nanomedicine and biomedical engineering. *Caspian J Intern Med.*, 5, 156–61. <https://dx.doi.org/10.PMC4143737>
- Gömeç, M., Sayın, K., Özkaraca, M. et al. (2022). Synthesis, In Silico and Investigation of Anti-Breast Cancer Activity of New Diphenyl Urea Derivatives: Experimental and Computational Study. *Journal of Molecular Structure*, 133414. <https://dx.doi.org/doi:10.1016/j.molstruc.2022.133414>
- Guo, C., Li, X., Wang, R. et al. (2016). Association between Oxidative DNA Damage and Risk of Colorectal Cancer: Sensitive Determination of Urinary 8-Hydroxy-2'-deoxyguanosine by UPLC-MS/MS Analysis. *Sci Rep*, 6, 1-9. <https://doi.org/10.1038/srep32581>.
- Han, H.J., Lee, J.S., Park, S.A. et al. (2015). Extraction optimization and nanoencapsulation of jujube pulp and seed for enhancing antioxidant activity. *Colloids and Surfaces B: Biointerfaces*, 130, 93-100. <https://dx.doi.org/doi:10.1016/j.colsurfb.2015.03.050>
- Howard, K.A., Paludan, S.R., Behlke, MA. et al. (2009). siRNA nanoparticle-mediated TNF-alpha knockdown in peritoneal macrophages for antiinflammatory treatment in a murine arthritis model. *Mol Ther*, 17, 162-8. <https://dx.doi.org/doi:10.1038/mt.2008.220>
- Jhaveri, J., Raichura, Z., Khan, T. et al. (2021). Chitosan Nanoparticles-Insight into Properties, Functionalization and Applications in Drug Delivery and Theranostics. *Molecules*, 26,272. <https://dx.doi.org/doi:10.3390/molecules26020272>
- Jovčevska, I., Muyldermans, S. (2020). The therapeutic potential of nanobodies. *BioDrugs Clin Immunotherap Biopharm Gene Therapy*, 34(1), 11-26. <https://dx.doi.org/10.1007/s40259-019-00392-z>.
- Keawchaon, L., Yoksan, R. (2011). Preparation, characterization and in vitro release study of carvacrol-loaded chitosan nanoparticles. *Colloids Surf. B: Biointerfaces*, 84, 163-171. <https://dx.doi.org/doi:10.1016/j.colsurfb.2010.12.031>
- Lee, S.I., Jeong, Y.J., Yu, A.R. et al. (2019). Carfilzomib enhances cisplatin-induced apoptosis in SK-NBE(2)-M17 human neuroblastoma cells. *Sci Rep.*, 9, 1-14. <https://doi.org/doi:10.1038/s41598-019-41527-0>.
- Li, J., Cai, C., Ja, L. (2018). Chitosan-Based Nanomaterials for Drug Delivery. *Molecules*, 23, 2661. <https://dx.doi.org/doi:10.3390/molecules23102661>
- Longacre, M., Snyder, N., Sarkar, S. (2014). Drug resistance in cancer: an overview. *Cancers*, 6, 1769-92. <https://dx.doi.org/doi:10.3390/cancers6031769>
- Mansoori, B., Mohammadi, A., Davudian, S. et al. (2017). The different mechanisms of cancer drug resistance: a brief review. *Tabriz Univ. Med. Sci.*, 7, 339-48. <https://dx.doi.org/doi:10.15171/apb.2017.041>
- Mittal, A., Singh, A., Benjakul, S. et al. (2020). Composite films based on chitosan and epigallocatechin gallate grafted chitosan: Characterization, antioxidant and antimicrobial activities. *Food Hydrocol*, 111, 1-10. <https://doi.org/10.1016/j.foodhyd.2020.106384>
- Mohammadi, A., Hashemi, M., Hosseini, S. (2015). Chitosan nanoparticles loaded with Cinnamomum zeylanicum essential oil enhance the shelf life of cucumber during cold storage. *Postharvest Biol. Technol.*, 110, 203-213. <https://doi.org/10.1016/j.postharvbio.2015.08.019>
- Park, W., Heo, Y.J., Han, D.K. (2018). New opportunities for nanoparticles in cancer immunotherapy. *Biomater Res.*, 22, 24-33. <https://dx.doi.org/10.1186/s40824-018-0133-y>.
- Purbowatiningrum, N., Ismiyanto, E.F. (2017). Cinnamomum casia Extract Encapsulated Nanochitosan as Antihypercholesterol. *IOP Conf Ser: Mater Sci Eng.*, 172, 012035. <https://dx.doi.org/doi:10.1088/1757-899X/172/1/012035>
- Robey, R.W., Pluchino, K.M., Hall, M.D. et al. (2018). Revisiting the role of efflux pumps in multidrug-resistant cancer. *Nat Rev Cancer*, 18, 452-64. <https://dx.doi.org/doi:10.1038/s41568-018-0005-8>.
- Salehi, B., Jornet, P.L., Lopez, E.P.F. et al. (2019). Plant-Derived Bioactives in Oral Mucosal Lesions: A Key Emphasis to Curcumin, Lycopene, Chamomile, Aloe vera, Green Tea and Coffee Properties. *Biomolecules*, 9(3), 1-23. <https://dx.doi.org/10.3390/biom9030106>.
- Sachdev, E., Tabatabai, R., Roy, V. et al. (2019). PARP Inhibition in cancer: An update on clinical development. *Target Oncol.*, 14, 657-79. <https://doi.org/doi:10.1007/s11523-019-00680-2>.
- Sharifi-Rad, M., Kumar, N.V.A., Zucca, P. et al. (2020). Lifestyle, oxidative stress, and antioxidants: back and forth in the pathophysiology of chronic diseases. *Front Physiol*. 11, 1-21. <https://dx.doi.org/10.3389/fphys.2020.00694>.
- Sima, P., Richter, J., Vetvicka, V. (2019). Glucans as new anticancer agents. *Anticancer Res.*, 39, 3373-78. <https://doi.org/doi:10.21873/anticancer.13480>.
- Singh, A., Benjakul, S., Prodpran, T. (2019a). Chitoooligosaccharides from squid pen prepared using different enzymes: characteristics and the effect on quality of surimi gel during refrigerated storage. *Food*

- Prod Process Nutri., 1, 1-10.
<https://doi.org/10.1186/s43014-019-0005-4>
- Singh, A., Benjakul, S., Prodpran, T. (2019b). Ultrasound assisted extraction of chitosan from squid pen: molecular characterization and fat binding capacity. *J Food Sci.*, 84, 224-234. <https://dx.doi.org/doi:10.1111/1750-3841.14439>.
- Tang, H., Zhang, Y., Li, D. et al. (2018). Discovery and synthesis of novel magnolol derivatives with potent anticancer activity in non-small cell lung cancer. *Eur J Med Chem*, 156, 190-205. <https://dx.doi.org/doi:10.1016/j.ejmech.2018.06.048>.
- Taşkın, D., Doğan, M., Ermanoğlu, M. et al. (2021). Achillea gonioccephala Extract Loaded into Nanochitosan: In Vitro Cytotoxic and Antioxidant Activity. *Clinical and Experimental Health Sciences*, 11(4), 659-666. <https://doi.org/10.33808/clinexphealthsci.972180>
- Taskin, T., Dogan, M., Yilmaz, B.N. et al. (2020). Phytochemical screening and evaluation of antioxidant, enzyme inhibition, anti-proliferative and calcium oxalate anti-crystallization activities of *Micromeria fruticosa* spp. brachycalyx and *Rhus coriaria*. *Biocatalysis and Agricultural Biotechnology*, 27, 1-7. 101670.
<https://doi.org/10.1016/j.bcab.2020.101670>
- Tavana, E., Mollazadeh, H., Mohtashami, E. et al. (2020). shRNA-VEGF: A promising phytochemical for the treatment of glioblastoma multiforme. *BioFactors*, 46, 356-366. <https://dx.doi.org/doi:10.1002/biof.1605>.
- Torabi, N., Dobakhti, F., Faghihzadeh S. et al. (2018). In vitro and in vivo effects of chitosan-praziquantel and chitosan-albendazole nanoparticles on *Echinococcus granulosus* Metacestodes. *Parasitol Res.*, 117, 2015–2023. <https://dx.doi.org/doi:10.1007/s00436>
- Urban-Klein, B., Werth, S., Abuharbeid, S. (2005). RNAi-mediated gene-targeting through systemic application of polyethylenimine (PEI)-complexed siRNA in vivo. *Gene Ther*, 12, 461-6.
<https://dx.doi.org/doi:10.1038/sj.gt.3302425>
- Wang, X., Zhang, H., Chen, X. (2019). Drug resistance and combating drug resistance in cancer. *Cancer Drug Resist.*, 2, 141-60.
<https://dx.doi.org/doi:10.20517/cdr.2019.10>
- Wang, R., Billone, P.S., Mullett, W.M. (2013). Nanomedicine in action: an overview of cancer nanomedicine on the market and in clinical trials. *J. Nanomater*, 1-12.
<https://doi.org/10.1155/2013/629681>
- Wikanta, T., Erizal, T., Tjahyono, T. et al. (2012). Synthesis of polyvinyl alcohol-chitosan hydrogel and study of its swelling and antibacterial properties. *Squalen Bulletin of Marine and Fisheries Postharvest and Biotechnology*, 7(1), 1-10.
- Xue, X., Liang, X.J. (2012). Overcoming drug efflux-based multidrug resistance in cancer with nanotechnology. *Chin J Cancer*, 31, 100-109.
<https://dx.doi.org/doi:10.5732/cjc.011.10326>
- Zitvogel, L., Apetoh, L., Ghiringhelli, F. et al. (2008). Immunological aspects of cancer chemotherapy. *Nat Rev Immunol*, 8(1), 59-73. <https://dx.doi.org/doi:10.1038/nri2216>.